Chemical amplifier, self-ignition mechanism, and amoeboid cell migration

M. Schienbein and H. Gruler*
Chaire Scientifique Roger Seydoux de la Fondation de France, Centre d'Écologie Cellulaire, Hôpital Pitié-Salpétrière, F75651 Paris, Cedex 13, France
(Received 10 February 1995; revised manuscript received 17 May 1995)

The signal transduction chain of amoeboid migrating cells, such as human granulocytes, is approximated. Only the mean concentration of intracellular messenger molecules is considered. The weak cellular input signal originating from membrane-bound receptors occupied by molecules that stimulate migration steers a large flux of energy and mass. The strong second intracellular signal is produced by a chemical amplifier. Several functions are performed by this second intracellular signal: (i) the activation of the microfilaments (linear motor), (ii) the renewal of the membrane-bound receptors, and (iii) the alteration of the input characteristics of the chemical amplifier. The rate equation for the second messenger is derived. The solution of this machine equation is compared with experimental results. The chemokinetic dose-response curve, as well as a machine cycle, are predicted. A threshold concentration of the migration-stimulating molecules is predicted. At high concentrations, the cells are in an activated state with self-maintained oscillations of the second intracellular messenger, and at low concentrations, the cells are in an inactivated state without oscillations. The migration-stimulated cells are compared to a laser.

PACS number(s): 87.10.+e, 87.22.Nf, 82.70.−y

INTRODUCTION

Interest in physical models of biological phenomena has grown considerably in recent years, and physicists are attracted by this interdisciplinary field. The physical approach is basically to treat a biological system as a physical state which is highly organized and complex, like a machine in which every part is more complex, more efficient, more precise, and much smaller than one is used to. The purpose of the present work is to show the analogy between a natural machine like a cell with its amoeboid movement induced by extracellular signal molecules, and man-made machines.

Many natural scientists are fascinated by the ability of single cells of the immune system to detect, respond to, and destroy microorganisms. Embryogenesis and wound healing are two of many examples where amoeboid movement plays a role [1,2].

An explanation of any biological processes is based on the maintenance of flux of energy and of matter through the systems [3]. The energy fed into the system in the form of chemical energy, whose processing involves many microscopic steps, eventually results in ordered phenomena on a macroscopic scale—for example, formation of macroscopic patterns in morphogenesis (self-organization of many migrating cells [4]) and migration of cells (self-organization of compartments within one cell [5]).

An important property of many biological organisms consists in their ability to actively move themselves through the medium. This motion is induced by processes which take place inside the living beings, which in turn represent open systems far from thermal equilibrium. The actual mechanisms of self-motion of even single living cells are considered to be very complicated [3].

Nonlinear dynamics is recognized as playing a crucial role in a wide variety of disciplines. The systems themselves may be physical, chemical, or biological, and the result is the spontaneous formation of new temporal and/or spatial macroscopic structures. This self-organization concept is clearly of particular relevance to complex systems both natural and artificial in origin. It is unfortunate so little progress has been achieved in the past towards the understanding of synchronization, pattern formation, and turbulence in nonlinear self-oscillatory media and related many-body systems, in spite of their great potential importance. The underlying physics is closely related to the slaving principles, whose conceptual importance in nonlinear dissipative dynamics in general was emphasized by Haken [3] and first demonstrated by his team in laser theory.

Artificial life is intended to display the essential properties of living beings without repetition of their biochemical material basis [6]. Our working concept—experimentally as well as theoretically—is to start with real cells such as human leukocytes: In the first step, the phenomenological equations for migration are experimentally established—a steerer for the speed and an automatic controller for the direction of migration [7,8]. Then, the essential cellular components for migration are experimentally determined [9,10]. The machinery which creates the cell locomotion contains only a few elements: a part of the plasma membrane, unstructured cytoplasm as seen by light microscopy, and the necessary biochemistry. These fragments (ghosts) change their shape continuously during the directed and nondirected amoeboid movement. The third step is of current interest: the steerer and the automatic controller are explained on the

*Permanent address: Abteilung bioPhysik, Universität Ulm, D89069, Ulm, Germany.

basis of the involved biochemical reaction chain.

It was shown for granulocytes, monocytes, somatic fibroblasts, and neural crest cells that two independently working cellular machines exist—a steerer and an automatic controller [7,11]. In fact, the migrating cells can be compared with a driven car where the speed, adjusted by the gas pedal, and the moving direction, adjusted by the steering wheel, can be independently altered.

Steerers and servo mechanisms are control systems in which a hydraulic, pneumatic, or other type of controlling mechanism is actuated and controlled by a low energy signal. In fact, steerer and servo mechanisms are as essential in biological systems as they are in modern technological society [12].

The cellular speed of granulocytes is generated by a steerer mechanism which is based on chemical reactions. The weak input signal originating from approximately 1000 membrane-bound receptors (high affinity receptors) occupied by molecules that stimulate migration, steers a large flux of energy and mass [13]. The result is an amplified output signal—the second intracellular signal which is responsible for the cellular speed. A process which will be discussed here. Our working hypothesis is that the total system can be viewed as an assembly of a large number of identical local systems which are coupled to each other.

SIGNAL TRANSDUCTION CHAIN

The basic biochemical reactions of the cellular signal transduction chain are essentially known [13–15], but the physical events are less understood. In Fig. 1 the chemical aspects (molecular approach) of the signal transduction chain as well as the physical aspects (machine description) are shown. First, we want to summarize what is known about the signal transduction chain of granulocytes [13].

One main function of the membrane is to separate the intracellular space from the extracellular space. In addition to this main function, the membrane is the first element in the signal transduction chain.

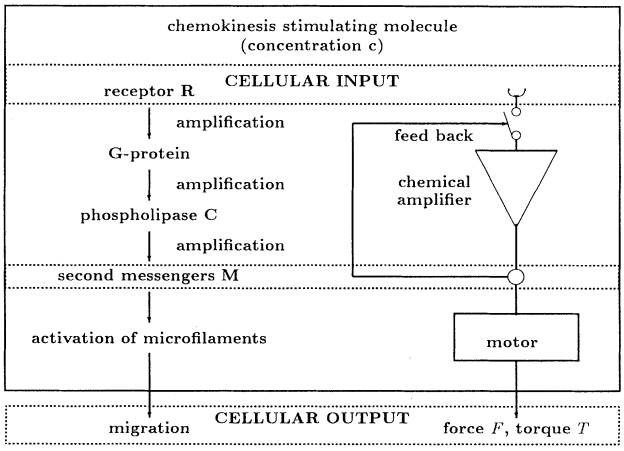

FIG. 1. Schematic representation of the cellular signal transduction-response chain. The chemical approach is shown on the left side and the physical approach on the right side.

Detection system and first intracellular messenger. Specific molecules, C, stimulating random locomotion (chemokinesis) and directed locomotion (chemotaxis) bind to the membrane-bound receptor, R, and create the first intracellular signal, R_C.

Amplification chain. The receptor complex, R_C, can be regarded as the first element in the biochemical amplification chain. One receptor complex, R_C, activates many membrane-attached G proteins. The activated G protein activates the phospholipase-C protein. One membrane-incorporated phospholipase-C protein hydrolyzes many ATP-activated phospholipid (phosphatidylinositol) molecules on the inner side of the membrane.

Second intracellular messengers. The water soluble head group inositol triphosphate opens calcium channels and intracellular calcium stores. Inositol triphosphate and calcium are regarded as the second cellular messengers. The increased concentration of second messengers triggers several functions:

(1) Linear motor. The amoeboid migration of the cell is induced by the second messenger triggered adhesion of the plasma membrane to a substrate and by the second messenger dependent activation of microfilaments (muscles).

(2) Self-ignition mechanism. Vesicles loaded with fresh receptors are forced to fuse with the plasma membrane. This fusion process is induced by the increase calcium concentration, the calcium concentration gradient close to the opened calcium channels, the concentration of the watersoluble inositol triphosphate, and the concentration of the membrane soluble diacylglycerol molecules [5,8]. The exposure of fresh receptors is the start of a new cycle.

Our approach to the signal transduction chain is actually a technical one. The right side of Fig. 1 could be a drawing for the machine shop to build a machine. The machine works far from thermal equilibrium even if it is not shown explicitly, e.g., an amplifier can only work far from thermal equilibrium since a weak input signal is used to control a large flux of energy and of mass to create the amplified output signal.

The linear motor and the chemokinetic dose-response curve

A simple technical description of the cellular signal transduction chain [16,17] predicts the chemokinetic dose-response curve. The rate equation for the cellular second messengers, M, is

$$\frac{dM}{dt}=k_t S-k_d M \ . \tag{1}$$

The first term describes the production rate of the intracellular second messenger. The cell is stimulated by signal molecules such as f-Met-Leu-Phe to produce intracellular second messengers. The occupancy of the membrane-bound receptors is regarded as the first intracellular signal, S. k_t is a signal transduction coefficient. The second term describes the decomposition of the

second intracellular messengers and k_d is a decay coefficient. The first intracellular signal is the fraction of occupied receptors,

$$S(c,t)=R_0(t)\frac{c}{c+K_R} . \quad (2)$$

The number of receptors, $R_0(t)$, is altered by a machine cycle which will be explained as follows: in the time interval $(0,t_1)$, R_0 receptors are exposed at the membrane and can be occupied by molecules of the extracellular space. No active receptors are available in the time interval (t_1,T), where T is the repetition time. The mean concentration of the second messenger, M, can be obtained by solving differential equation (1) for the two time intervals,

$$M=\mathcal{A}\frac{c}{c+K_R} . \quad (3)$$

$\mathcal{A}$ is essentially constant when $k_d t_1 < 1$. The second intracellular messenger activates the microfilaments of the linear motor where traction is produced by converting chemical energy into mechanical work. The produced line tension (traction), $\sigma_\parallel$, at the leading edge can be approximated by the following expression:

$$\sigma_\parallel=K_A\mathcal{A}\frac{c}{c+K_R}-K_D v . \quad (4)$$

The first term describes the maximum traction which is assumed to be proportional to the second messenger. K_A is a signal transduction coefficient. The second term describes that the construction work of the cellular linear motor is more difficult under speed. This process is quantified by an intrinsic motor friction coefficient, K_D.

The linear motor of granulocytes can be investigated in the following way: A cell migrating in a narrow tube is forced to stop by applying counter pressure. The experimental result is approximated by the following equation [18]:

$$\sigma_\parallel=\sigma_\parallel^0(1-\alpha v) \quad (5)$$

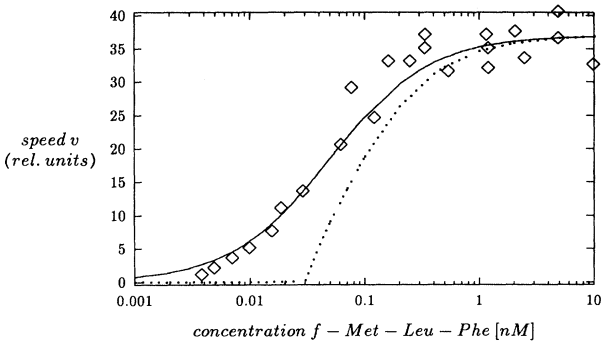

FIG. 2. Chemokinetic dose-response curve of granulocytes stimulated by signal molecule f-Met-Leu-Phe (tripeptide) of the extracellular space. The dots are experimental data from Ref. [36]. The line is a prediction of the simple model [Eq. (6) with $K_R=0.04$ nM]. The dotted line is a prediction of the more realistic model of the cellular signal transduction chain [Eq. (34) with $K_R=0.04$ nM].

with $\sigma_\parallel^0$ $(=K_A\mathcal{A})=2.0\pm0.18$ mN/m and $v_{\max}=\alpha^{-1}$ $(=\mathcal{A}K_A/K_D)=0.14\pm0.04$ μm/s for $c>K_R$. The intrinsic friction coefficient, K_D, of the motor is then 14 ± 4 kPa s.

The mean cellular speed of granulocytes is predicted as

$$v=\mathcal{A}\frac{K_A}{K_D}\frac{c}{c+K_R}=v_{\max}\frac{c}{c+K_R} \quad (6)$$

since the friction between the cell body and the substrate is negligible [18]. The measured chemokinetic dose-response curve as shown in Fig. 2 exhibits the predicted behavior. The total number of occupied receptors, representing the first intracellular signal, is proportional to the cellular speed.

This simple approximation of the signal transduction chain serves to explain the linear motor and the chemokinetic dose-response curve. In the next step we will show the essential steps in the signal transduction chain for predicting the periodic temporal variations of the receptors and the second intracellular messenger.

Machine cycle

Our working hypothesis is that the increases in the concentrations of second messengers such as calcium and the hydrolyzed products (inositol triphosphate and diacylglycerol) are the stimuli for the fusion of the vesicles with the plasma membrane [5]. Thus, we are dealing with a self-ignition machine like a Diesel engine. The measured delay time between the application of an extracellular signal and the formation of intracellular signals that are responsible for the establishment of fresh receptors, is essential for the self-ignition mechanism.

For granulocytes the following experimental facts are in accordance with our working hypothesis:

(i) The predicted lag time between signal application and cellular response (formation of a new leading front) has been measured. It was approximately 10 s for chemotaxis (micropipet) [19], 8–10 s for necrotaxis (Fig. 3), and 8–10 s for galvanotaxis [20,21].

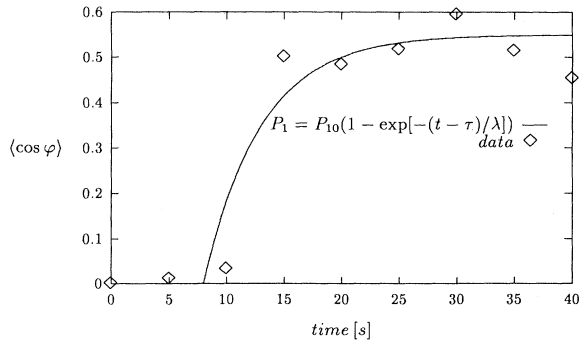

FIG. 3. Necrotactic field-jump experiment [37]: The polar order parameter, $\langle\cos\varphi\rangle$, as a function of time t is shown. The central symmetric cellular guiding field was switched on at $t=0$ when an erythrocyte in the center of the viewing field was lysed by a light pulse (ruby laser). The first cellular response was observed after a lapse time of 8–10 s ($\tau=8$ s).

(ii) The predicted intracellular cycle can be determined by measuring the rhythmic fluctuations of the electric transmembrane potential difference with a microelectrode (Fig. 4) [22].

(iii) The existence of the cellular cycle can be shown by applying periodic extracellular signals (Fig. 5) [21]: The intracellular cycle can be slaved by the extracellular signal. It was possible to synchronize granulocytes by short electric pulses (0.8 V/mm for 1 s) with a repetition time of a multifold of 8 s.

(iv) The shape of migrating granulocytes showed rhythmic undulations with a characteristic time of 10 s [23].

(v) The shape of suspended granulocytes showed rhythmic oscillations with a characteristic time of 8 s [24,25].

The experimental data shown support a cyclic component in the overall mechanism of granulocyte motility with a characteristic time of 8 to 10 s. Next, the cyclic working signal transduction chain will be derived by considering more details of the biochemical reactions.

Detection system

The first step in the signal chain of the cellular machine is the provision of new receptors, R, in the membrane. The rate equation for this process is approximated by the following equation:

$$\frac{dR}{dt}=k_f F(M)-k_{1e}R-k_{11}Rc+k_{22}R_C \ . \tag{7}$$

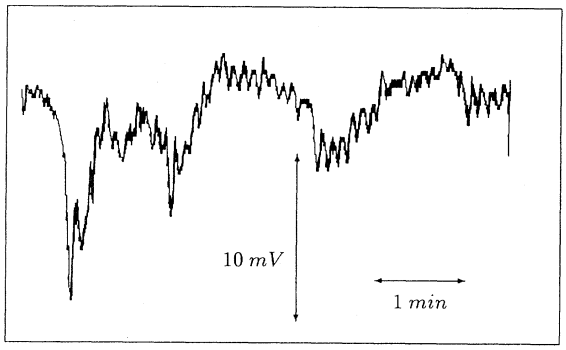

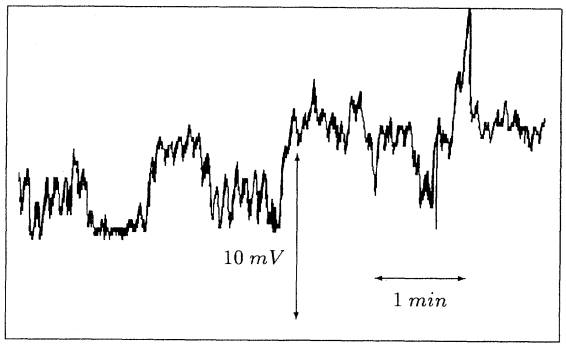

FIG. 4. A typical membrane potential difference as a function of time is shown [22]. Two characteristic times can be seen: $T_1=8$ s and $T_2=60-80$ s.

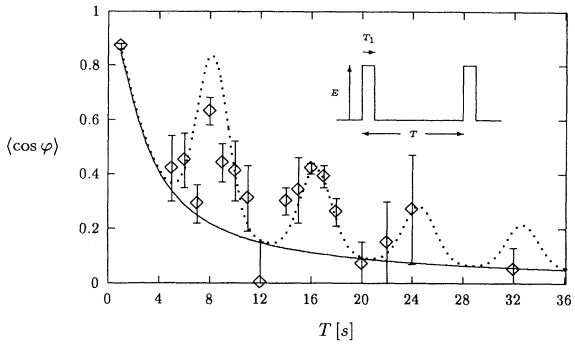

FIG. 5. The steady state polar order parameter of granulocytes exposed to pulsed electric guiding fields ($E=0.8$ V/mm, $T_1=1$ s) as a function of repetition time T is shown [21]. The line is a prediction [8]. [The values of the machine coefficients were obtained from quantification of the random walk (mean-squared displacement vs time) and quantification of the directed movement (polar order parameter vs applied polar guiding field)]. The dotted line is obtained for synchronized cells.

The first term describes the fusion of vesicles with new receptors, with the plasma membrane. The fusion process is assumed to be triggered by the signal molecules coming out of the chemical amplification chain—the second intracellular messengers, M. The inactivation of the receptors is described by the second term. The next terms describe the binding of a chemoattractant molecule with concentration c at a receptor with concentration, R. This binding process is regarded as reversible.

The renewal of receptors is considered as a process with a high cooperativity. Which means, e.g., not only one type of second messenger is involved but several types such as calcium and inositol triphosphate ions and diacylglycerol molecules. The unknown vesicle fusion function, $F(M)$, may be approximated by the following analytical expression [26] (Fig. 6):

$$F(M)=\frac{M^n}{K_f^n+M^n} \ . \tag{8}$$

It is assumed that n different types of second messengers

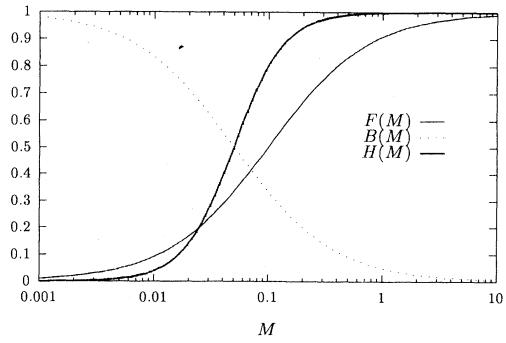

FIG. 6. The function $F(M)$ (vesicle fusion process), the function $B(M)$ (amplifier characteristics), and the decay function $H(M)$ (second messenger decay) as a function of the second intracellular messenger M are shown.

are involved with the same sensitivity (M is measured in units of K_f). For example, (i) the water soluble second messengers such as calcium and inositoltriphosphate, can induce vesicle fusion; (ii) the remaining lipid diacylglycerol with its uncharged small polar head as well as the ion flux through the calcium channel are involved in the fusion process.

The rate equation for the chemoattractant-receptor complex, R_C, is then

$$\frac{dR_C}{dt}=k_{11}Rc-k_{22}R_C-k_{2e}R_C \ . \tag{9}$$

The first two terms describe the binding dynamics of the chemoattractant molecule to the receptor. The inactivation of the occupied receptors is described by the third term.

The temporal behavior of the cellular detection system can be predicted by solving the following system [Eqs. (7) and (9)]:

$$\frac{d}{dt}\begin{bmatrix} R \\ R_C \end{bmatrix}=\begin{bmatrix} a_{11} & a_{12} \\ a_{21} & a_{22} \end{bmatrix}\begin{bmatrix} R \\ R_C \end{bmatrix}+k_f\begin{bmatrix} F(M) \\ 0 \end{bmatrix} \tag{10}$$

with

$$a_{11}=-(k_{11}c+k_{1e}) \ ,$$
$$a_{12}=k_{22} \ ,$$
$$a_{21}=k_{11}c \ ,$$
$$a_{22}=-(k_{22}+k_{2e}) \ .$$

The eigenvalues

$$\lambda_1=-(k_{11}c+k_{22}), \quad \lambda_2=-(k_{1e}+k_{2e}) \tag{11}$$

are obtained from the homogeneous equation

$$\begin{vmatrix} a_{11}-\lambda & a_{12} \\ a_{21} & a_{22}-\lambda \end{vmatrix}=0 \ . \tag{12}$$

The temporal changes of the number of receptors, $R(t)$, and of receptor-complexes, $R_C(t)$, are (see Appendix A)

$$R(t)=k_f\int_0^t\left[\frac{a_{21}\exp[\lambda_1(t-t')]+a_{12}\exp[\lambda_2(t-t')]}{a_{12}+a_{21}}\right]F(M)dt' \ , \tag{13}$$

$$R_C(t)=k_f\int_0^t\left[\frac{a_{21}\exp[\lambda_1(t-t')]-a_{21}\exp[\lambda_2(t-t')]}{a_{12}+a_{21}}\right]F(M)dt' \ . \tag{14}$$

The temporal evolution of R and R_C is governed by the two eigenvalues λ_1 and λ_2. One of them, λ_1, describes purely the fast kinetics of the ligand binding process ($\ll s$) [27]. The other one, λ_2, is the slow inactivation process of the receptors (R and R_c) (in the order of s) [14].

Adiabatic approximation. The temporal evolution of the vesicle fusion as described by $F(M)$ should slowly vary in time compared with the ligand binding process as described by $\exp[\lambda_1 t]$. The temporal change of the membrane-bound receptors, $R(t)$, then reads in case of the simplification $2k_e=k_{1e}+k_{2e}$.

$$R(t)=F(M)\left[\frac{k_f}{2k_e}\frac{k_{22}+k_e}{k_{22}+k_{11}c}-k_f\frac{a_{12}}{a_{12}+a_{21}}\frac{e^{\lambda_2 t}}{\lambda_2}\right] . \tag{15}$$

An adiabatic approximation can be used if the receptor loading kinetic is fast compared with the temporal variations of the receptor density. If this holds true, only the steady state concentrations for both $R^{\rm st}$ and $R_C^{\rm st}$ have to be considered. One obtains (see Appendix B)

$$R^{\rm st}=F(M)\frac{k_f}{2k_e}\frac{K_R+\dfrac{k_e}{k_{11}}}{K_R+c} \ , \tag{16}$$

$$R_C^{\rm st}=F(M)\frac{k_f}{2k_e}\frac{c}{c+K_R} \tag{17}$$

with $K_R=k_{22}/k_{11}$. The second equation is formally identical with Eq. (2) which is obtained from the model of the simple signal chain approximation. But the temporal variations of the receptors are predicted by the more complex model of the signal chain

$$R_0(t)=F(M)\frac{k_f}{2k_e} \ . \tag{18}$$

As expected, the total number of receptors is given by the fraction of the vesicle fusion rate, $k_fF(M)$, and of the receptor inactivation rate, $2k_e=k_{1e}+k_{2e}$.

Amplification chain

The chemical amplification chain in the cellular signal transduction chain is a sequence of chemical reactions where the first intracellular messenger, $S_{\rm in}$ ($=R_C$), starts the reaction.

$$S_{\rm in}\rightarrow S_1\rightarrow S_2\rightarrow\cdots\rightarrow S_N=S_{\rm out} \ . \tag{19}$$

A Fokker-Planck equation can be used to approximate the chemical amplification chain as it is shown in Appendix C. A matrix notation is used below:

$$\frac{d\vec{S}}{dt}=\mathcal{A}\vec{S}+\vec{B} \tag{20}$$

with

$$\vec{S}=\begin{bmatrix} S_1 \\ \cdots \\ \cdots \\ \cdots \\ S_N \end{bmatrix},\quad \mathcal{A}=\begin{bmatrix} -(f_1+b_1) & b_2 & 0 & 0 & \cdots \\ f_1 & -(f_2+b_2) & b_3 & 0 & \cdots \\ \cdots & \cdots & \cdots & \cdots & \cdots \\ \cdots & \cdots & \cdots & \cdots & \cdots \\ 0 & 0 & \cdots & f_{N-1} & -(f_N+b_N) \end{bmatrix},\quad \vec{B}=\begin{bmatrix} k_b S_{\text{in}}(M)B(M) \\ 0 \\ \cdots \\ \cdots \\ 0 \end{bmatrix}.$$

The chemical reaction chain can be described by forward reaction coefficients, f_i, and backward reaction coefficients, b_i. To simplify the mathematical expressions, all forward reactions are approximated by one coefficient, f_0, and all backward reactions by one coefficient, b_0.

The input signal, $S_{\text{in}}(M)$, and the amplifier characteristics, $B(M)$, are functions of the second intracellular signal. The amplification chain is based on enzymatic reactions which can be inhibited or enhanced by specific molecules. The second intracellular messenger molecules can be regarded as such specific molecules. For example, two types of ions may be involved—the calcium and the inositol triphosphate ions. This idea will be introduced here in a simplified way: Only the first reaction in the signal chain is assumed to be a function of the concentration of the second intracellular messengers, M. The unknown amplifier characteristic, $B(M)$, may be approximated by the following analytical expression [28,29] (Fig. 6):

$$B(M)=\left[1-\frac{M^q}{K_b^q+M^q}\right]=\frac{K_b^q}{K_b^q+M^q}\ . \tag{21}$$

The cooperativity is described by the number q of involved different types of second messenger molecules (M is measured in units of K_b).

In more technical terms, $B(M)$ represents the input characteristic of the amplifier when multiplied with the signal S_{in} coming out of the detection unit, and results in the input signal $G(M(t))[=k_b S_{\text{in}}(M)B(M)]$ which depends on the concentration of the second messenger M. The vesicle fusion process, $F(M)$, as well as the input characteristic of the amplifier, $B(M)$, represents possible feedback mechanisms.

The above mentioned set of rate equations (20) can be solved in the following way: A new variable, p, is introduced by using the Laplace transformation. The input signal and the signal within the amplifier then reads

$$\mathcal{G}(p)=\int_0^\infty e^{-pt}G(t)dt\ , \tag{22}$$

$$\mathcal{S}_i(p)=\int_0^\infty e^{-pt}S_i(t)dt,\quad i=1,\ldots,N\ . \tag{23}$$

For simplicity, we assume that the backward reaction can be neglected with respect to the forward reaction ($f_0 \gg b_0$). The signal within the amplifier is described by

$$(p+f_0)\mathcal{S}_1=\mathcal{G}(p)\ , \tag{24}$$

$$(p+f_0)\mathcal{S}_2=f_0\mathcal{S}_1\ , \tag{25}$$

$$\vdots \tag{26}$$

$$p\mathcal{S}_N=f_0\mathcal{S}_{N-1}\ . \tag{27}$$

N describes the number of elementary steps in the chemical amplification chain. This system of equations can easily be solved, and we obtain for the signal, $\mathcal{S}_N(p)$, coming out of the chemical amplifier

$$\mathcal{S}_N(p)=\frac{f_0^{N-1}}{(p+f_0)^N}\mathcal{G}(p)\ . \tag{28}$$

The time-dependent output signal is obtained by making the back transformation of Eq. (28) (convolution theorem)

$$S_N(t)=\frac{f_0^{N-1}}{(N-1)!}\int_0^t t'^{(N-1)}\exp[-f_0t']G(M(t-t'))dt'\ . \tag{29}$$

The signal $S_N(t)$ coming out of the amplification chain can be explained in the following way: (i) The amplification is described by the factor in front of the integral. (ii) The change between input and output signal is described by the integral. The output signal is a function of the input signal $G(M(t-t'))$, and the concentration of the second messenger M, at previous times $t-t'$ where the Poisson distribution

$$p(N-1,t)=\frac{t^{(N-1)}}{(N-1)!}\exp[-f_0t] \tag{30}$$

is the weight function. The time lag, $T(=N/f_0)$, between the input and output signal is an important property of the chemical amplifier.

Second intracellular messenger

The second intracellular messengers are formed in the last step of the amplification chain:

$$\frac{dM}{dt}=f_0S_N(M(t-t'))-H(M)\ . \tag{31}$$

The first term on the right-hand side describes the output signal of the chemical amplification chain. The second term describes the decay of the second messenger. The unknown decay function, $H(M)$, may be approximated by following analytical expression [28,29] (Fig. 6):

$$H(M)=d_h M+k_h \frac{M^r}{K_h^r+M^r} . \tag{32}$$

Chemical reactions and the action of ion pumps can decease the second messengers. These actions are described by the first term. The second term describes processes like adsorption or flux through ion channels. The cooperativity is described by r (signal transduction coefficients d_h and k_h; M is measured in units of K_h).

The final rate equation for the evolution of the second messenger is obtained from Eq. (31) by inserting Eqs. (29) and (32):

$$\frac{dM}{dt}=\frac{f_0^N}{(N-1)!}\int_0^t t'^{(N-1)}\exp[-f_0 t'] \times G(M(t-t'))dt'-H(M) . \tag{33}$$

The first term on the right-hand side describes the gain and the second term the loss. This equation can be simplified by introducing a dimensionless time, $t^*=f_0 t$ (in subsequent equations t means the new time where the asterisk is omitted):

$$f_0\frac{dM}{dt}=\frac{1}{(N-1)!}\int_0^t t'^{(N-1)}\exp[-t']G(t-t')dt' -H(M) . \tag{34}$$

This equation approximates more accurately the cellular signal transduction chain than the above shown simple approximation [Eq. (1)]. Only one equation has to be discussed in case of the adiabatic limit. Otherwise, Eq. (34) in connection with Eq. (14) have to be solved.

At first glance, it seems that the more accurate approximation of the signal transduction chain leads to a very complex model where many assumptions were used. But there are only four crucial properties:

(i) Detection: The first intracellular signal are the membrane-bound receptors loaded with kinesis stimulating molecules of the extracellular space.

(ii) Inertia: The signal coming out of the chemical amplification chain is delayed with respect to the input signal.

(iii) Feedback: The receptor supply and the input characteristic of the amplifier are functions of the second messenger from previous times.

(iv) Deactivation: The second messengers are deactivated.

SELF-IGNITION MACHINE

As we have shown above, the cellular signal transduction chain can be split into three parts: (i) the first intracellular messenger, (ii) the chemical amplifier, and (iii) the second intracellular messenger. The self-ignition machine is discussed in the adiabatic approximation. Thus, only the highly nonlinear differential equation [Eq. (34)] has to be investigated which will be solved numerically. Choosing appropriate values for the coefficient, oscillations in the receptor density as well as in the concentration of the second intracellular messenger, M, are obtained.

Next, the transition between the oscillatory and nonoscillatory states will be investigated. The nonlinear differential equation will be linearized.

Stability analysis

In the first step, the steady state of the nonoscillatory state is considered. The steady state value of the second intracellular messenger may be M_0. Taylor series close to the steady state value are taken for the gain function, $G(M)$, and the loss function , $H(M)$:

$$G(M)=G(M_0)+\left.\frac{\partial G}{\partial M}\right|_{M_0}(M-M_0)+\cdots , \tag{35}$$

$$H(M)=H(M_0)+\left.\frac{\partial H}{\partial M}\right|_{M_0}(M-M_0)+\cdots . \tag{36}$$

In the case of steady state ($dM/dt=0$, $M-M_0=0$), Eq. (34) then reads

$$G_0 P(N,t)-H_0=0 \tag{37}$$

with the incomplete gamma function, $P(N,t)$, of order N:

$$P(N,t)=\frac{1}{(N-1)!}\int_0^t t'^{(N-1)}\exp[-t']dt' \tag{38}$$

and the abbreviations

$$G_0=G(M_0)=k_g i(c)F(M_0)B(M_0) , \tag{39}$$

$$H_0=H(M_0) \tag{40}$$

with

$$k_g=\frac{k_b k_f}{2k_e} , \tag{41}$$

$$i(c)=\frac{c-\frac{k_e}{k_{11}}}{K_R+c} . \tag{42}$$

The gain term, G_0, is modulated by basically the first intracellular signal $i(c)$.

The signal chain for large time t is of interest. Thus, Eq. (37) can be simplified since each incomplete gamma function $P(N,t)$, $N\geq 1$ tends to 1 for $t\rightarrow\infty$ (Fig. 7). One obtains

$$G_0-H_0=0 , \tag{43}$$

where the gain equals the loss. To solve this equation, one needs actual values for the assumed gain function, $G(M_0)$, and the loss function, $H(M_0)$. The calculations are performed with the following values: $k_R=2$, $k_{11}=10$, $k_e=1/10$, $k_g=10$, $k_h=2$, $d_h=1/10$, $K_f=1/10$, $K_b=5/100$, $K_h^2=5/100$, $f_0=1$, $q=n=1$, $r=2$. Two solutions, $M_{01}(=0)$ and M_{02}, are found as can be seen from Fig. 8. The first one is unstable because

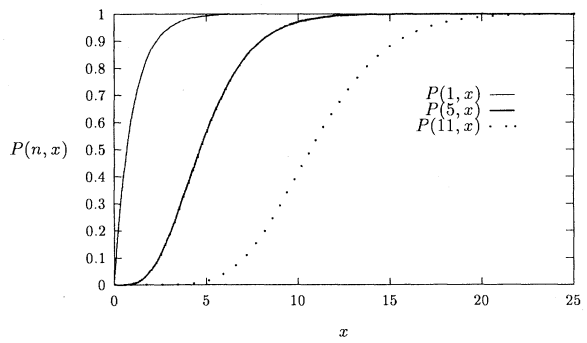

FIG. 7. The incomplete gamma functions, $P(n,x)$, as a function of x are shown for different $n(=1,5,11)$.

$$\left.\frac{\partial(G-H)}{\partial M}\right|_{M_{01}}>0 \tag{44}$$

and therefore of less interest. But the second one is stable because

$$\left.\frac{\partial(G-H)}{\partial M}\right|_{M_{01}}<0\ . \tag{45}$$

The main task is to find out under which conditions the state M_{02} becomes unstable.

The essential quantity which can alter the stability is the concentration, c, of the chemokinesis-stimulating molecule in the environment of the cell since the term, G_0, is proportional to $i(c)$ [see Eqs. (39) and (42)]. The system performs oscillations at large c and is stable at small c. At the critical concentration, c_c, the cellular state alters from a stable state to an oscillating state.

Next, Eq. (34), which describes the signal transduction chain, will be linerized and analyzed in respect to its stability. A linear equation in respect to $m(t)[=M(t)-M_0]$ is obtained (see Appendix D),

$$f_0\frac{dm}{dt}=G_0P(N,t)+G_0'm(t-N)-[H_0+H_0'm(t)]\ , \tag{46}$$

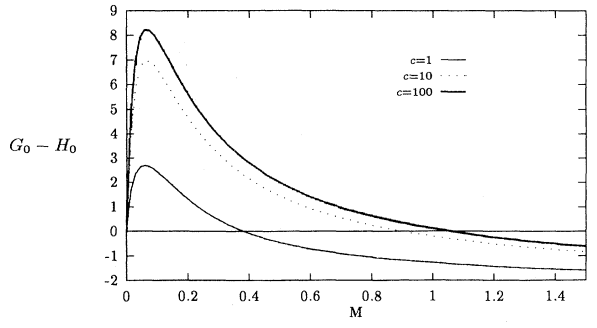

FIG. 8. The function G_0-H_0 is plotted vs M for different concentration c. The steady state is obtained for $G_0-H_0=0$. One solution, M_{01}, is obtained for $M=0$. The value of the second solution, M_{02}, depends on the concentration c.

with $H_0'=\partial H/\partial m|_{M_0}$. It is not necessary to consider this inhomogeneous differential equation since the kinetics is already described by the homogeneous equation:

$$f_0\frac{dm}{dt}=G_0'm(t-N)-H_0'm(t)\ . \tag{47}$$

The basic features of the cellular signal transduction chain are described by this differential equation. The temporal variations of the second messenger (left-hand side of equation) depends on the production rate (first term on right-hand side) and the loss rate (second term). The linearized production function, $G(M)$, depends on (i) the receptor supply, (ii) the fraction of occupied receptors, and (iii) the amplifier characteristics. In the present model it is assumed that the receptor supply function, $F(M)$, and the amplifier characteristics, $B(M)$, are functions of the second messengers. The occurrence of the oscillating state is not very sensitive to the chosen functions, $F(M)$ and $B(M)$ (gain), and $H(M)$ (loss).

We are looking for the condition where a nonoscillatory state is altered to an oscillatory state [30]. The solution of the linear differential equation (47) is

$$m(t)=m_0e^{\lambda t}\ . \tag{48}$$

A transcendental algebraic equation is obtained if Eq. (48) is introduced into (47),

$$\tilde{\lambda}=G_0'\exp[-\tilde{\lambda}T]-H_0'\ , \tag{49}$$

with the new quantity $\tilde{\lambda}=f_0\lambda$ and the delay time $T=N/f_0$. The complex number, $\tilde{\lambda}$, can be split into its real and imaginary part $(\mu+i\omega)$ and one obtains from Eq. (49) an equation for the real and another one for the imaginary part:

$$\mu=G_0'e^{-\mu T}\cos\omega T-H_0'\ , \tag{50}$$

$$\omega=-G_0'e^{-\mu T}\sin\omega T\ . \tag{51}$$

For $\mu<0$ the system reaches a stable state (damped oscillations) but for $\mu>0$ the amplitude of the oscillations increases with time. Thus, a critical condition is reached if the real part vanishes. The following two equations are obtained for $\mu=0$:

$$\frac{\omega}{H_0'}+\tan\omega T=0\ , \tag{52}$$

$$G_0'^2-H_0'^2+\omega^2=0\ . \tag{53}$$

These equations can be solved in the following way. First ω as a function of M_0 is calculated from Eq. (52), (note H_0' is a function of M_0). Then, ω is inserted into Eq. (53). A rootfinding technique is used to determine the value of M_0 where Eq. (53) hold true. Typical results are shown in Figs. 9 and 10. In Fig. 9 the function $G_0'^2-H_0'^2+\omega^2$ of Eq. (53) is shown for different delay times T. Note, the chemical amplification factor, N, is proportional to delay time $T(=N/f_0)$. The value M_0, where $G_0'^2-H_0'^2+\omega^2$ equals zero, is large for small delay times T. The critical concentration, c_c, is finally obtained from Eq. (43). By varying c and finding the second root of Eq. (43), we obtain the curve shown in Fig. 10, where M_0 is plotted

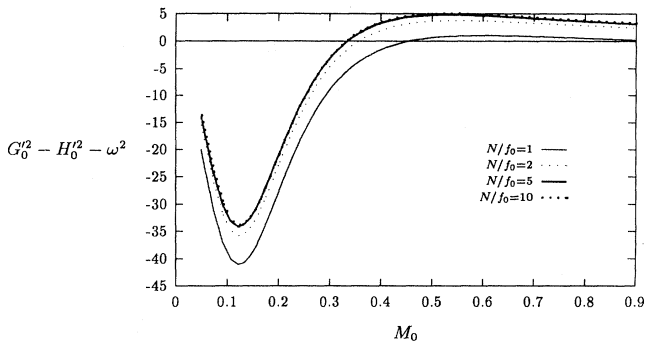

FIG 9. The function $G_0'^2 - H_0'^2 - \omega^2$ is plotted vs M_0 for various N. For large N the intersection ($G_0'^2 - H_0'^2 - \omega^2 = 0$) tends to a limit value M_0.

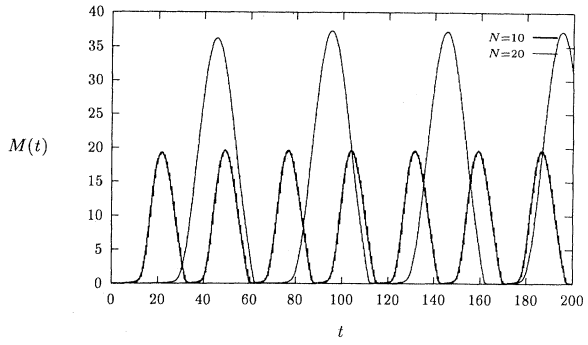

FIG 11. Numerical solutions of the model system are shown. The second messenger $M(t)$ is calculated as a function of time. The calculations are made for high concentration ($c=1000$). The influence of the chemical amplifier on the second messenger is demonstrated for two values of $N(=10,20)$.

versus the concentration c. For large amplitude ($N \to \infty$), the critical concentration approaches a small finite concentration value (≈ 0.78). For low amplification (e.g., $N=1$), the critical concentration is high (≈ 1.35).

It was shown by means of the linearized differential equation (46) that there exists a transition between an oscillatory and a nonoscillatory cellular state which is driven by the concentration, c, of the kinesis stimulating molecules.

In the next step, the amplitudes of the oscillations are calculated. In this case the nonlinearizled differential equation (34) has to be solved. The amplitudes of the second messenger, $M(t)$, the receptors, $R(t)$, and the occupied receptors, $R_C(t)$, are calculated as a function of time. Typical results are shown in Figs. 11 and 12. The calculated second intracellular messenger, $M(t)$, oscillates in time as shown in Fig. 11. The onset of the oscillations takes place after a lapse time, t_{on}, which is approximately the delay time in the amplification chain N/f_0. $M(t)$ is calculated for two different values of amplification N. It demonstrates that the period grows by a factor ≈ 2 if the amplification, N, is doubled. The calculated oscillation of the receptor, $R(t)$, and receptor complex, $R_C(t)$, concentrations are shown in Fig. 12.

To compare numerical results with the linear stability analysis one has to change the concentration c and to see if there are still oscillations visible in $M(t)$. The upper part of Fig. 13 shows the exponential decay of the oscillation amplitude as a function of time. Thus, the system exhibits no oscillation for large times t. The lower part of Fig. 13 shows $M(t)$ if the concentration is slightly increased. The oscillation amplitude decays exponentially to a finite value. Thus, the system exhibits oscillation for large times where its amplitude is independent of the starting value. In Fig. 14 the amplitude of the oscillating second intracellular messenger (cellular output A) is shown as a function of concentration, c, and of the amplification factor, N. A threshold behavior is demonstrated. For small concentrations , $c < c_c$, the oscillation amplitude of the second intracellular messenger is zero. The cell is in a stable state—no migration is expected. For large concentrations, $c > c_c$, the oscillation amplitude of the second intracellular messenger is finite. The cell is in an oscillatory state—migration is expected. The critical concentration is also a function of the amplification as already shown. The critical concentration, c_c, decreases from ≈ 3.5 ($N=1$) to ≈ 0.8 ($N \to \infty$) if the amplification factor, N, is increased.

Experimental verifications

Our approximation of the cellular signal transduction chain (detection system—first intracellular messenger—

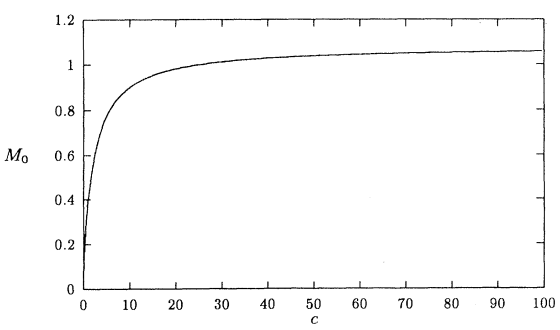

FIG. 10. The steady state value M_0 vs the concentration c is shown. The numbers are given in relative units.

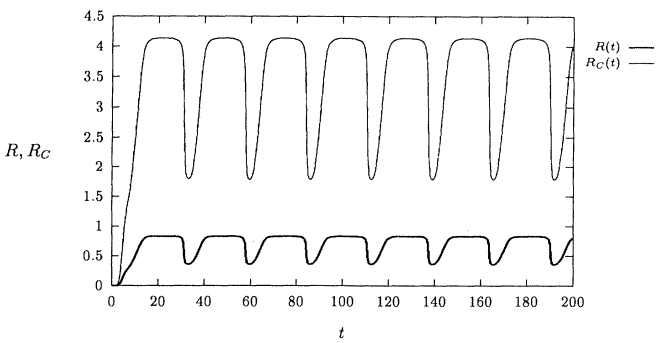

FIG. 12. The receptor R and receptor-complex R_C are calculated as a function of time ($c=10$ and $N=10$).

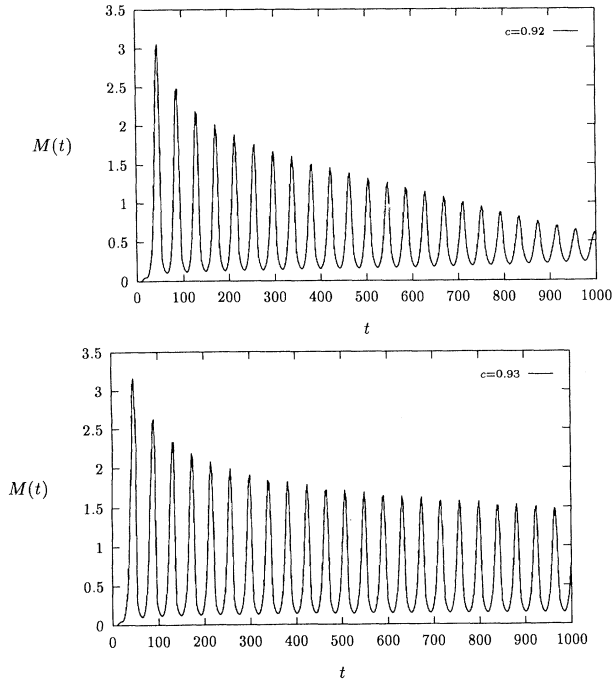

FIG. 13. The second messenger $M(t)$ is shown as a function of time. The oscillating amplitude decays to zero for large times as seen in the upper part of the figure ($c < c_c$) and to a finite value as seen in the lower part of the figure ($c > c_c$).

chemical amplifier—second intracellular messenger—feedback to the detection system and the chemical amplifier) leads to self-maintained oscillation in the cellular signal transduction chain. The oscillations could be detected on a molecular level or on a macroscopic level where cellular functions are investigated.

(i) The self-ignition model for cellular migration is based on biochemical reaction which takes place in and at the cellular membrane. No further cellular elements

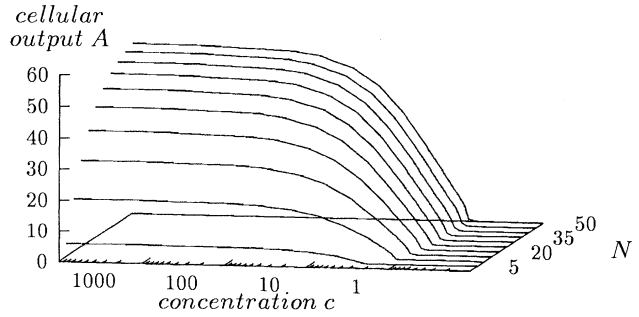

FIG. 14. The oscillating part of the second messenger (z direction) is shown as a function of the concentration c of the kinesis stimulating molecules (x direction) and of the chemical amplification N (y direction) (start $N=5$, increment $\Delta N=5$). For small concentrations, $c < c_c$, the cellular state is stable—no oscillation and no migration. For large concentrations, $c > c_0$, the cellular state is unstable—the cells perform oscillation and the cells migrate.

are used. The existence of cytokineplasts (ghosts) prepared out of granulocytes is a strong support of the model since the ghosts contain no visible cellular structure but still have the ability to perform directed and nondirected migration [9,10]. These ghosts have a rhythm with a characteristic time of 8–10 s as can be measured by the cross-correlation function between the projected area and the speed [32]. For ghosts and whole cells, the same rhythm is predicted as actually observed.

(ii) One prediction of the model is that the second intracellular signal should show oscillations. Intracellular calcium is regarded as one important second intracellular messenger which can easily be detected. One of our current projects is to find oscillations in granulocytes with an 8 s periodicity; however, up to now we have not been successful [31].

(iii) The predicted rhythm in the detection cycle is proved by the ability to synchronize cells by periodically applied extracellular signals with a repetition time of a multifold of 8 s [21].

(iv) One prediction of the model is that there exists a lapse time between signal recognition and cellular response. This lapse time should be approximately the repetition time of the oscillations. In granulocytes the repetition time was measured to be approximately 8 s. The measured lapse time is approximately 8–10 s.

(v) One prediction of the model is that the fluctuation-dissipation theorem does not hold since the cell cannot receive continuous external signals. The cell can only receive extracellular signals in well defined time increments with respect to the predicted internal rhythm (see Fig. 12). The experimental proof of the failure of the fluctuation-dissipation theorem takes place in several steps: First, fluctuation experiments are performed as (i) random walks and (ii) directed migrations with a constant guiding field (the trajectories fluctuate around the desired direction). Second, these fluctuation experiments are quantified [8]. Third, a guiding field-jump experiment is predicted by using the values obtained from the fluctuation experiments, e.g., a relaxation time of 20–30 s is expected. Fourth, a guiding field-jump experiment is performed. The actual measured relaxation time is 42 s—much longer than predicted. The fluctuation-dissipation theorem failed due to the intracellular measuring cycle [8].

Next, the measured chemokinetic dose-response curve will be compared with model predictions.

Dose-response curve

The simple approximation of the signal transduction chain (receptor-ligand kinetics, one reaction step for the amplifier, speed proportional to second messenger, no feedback) describes quite well the measured chemokinetic dose-response curve. Receptor occupancy is obviously the essential event for explaining the cellular response. The signal transduction chain is approximated more realistically in the new model (receptor-ligand kinetics, several reaction steps for the amplifier, speed proportional to second messenger, feedback to receptor supply and/or amplifier). The predicted dose-response curve is calculated in the following way: First, the second intra-

cellular messenger, $M(t)$, is calculated as a function of time, t, at a given concentration, c. The oscillation amplitude of M is determined for long t. The cellular speed is expected to be proportional to the concentration of the second intracellular messenger. This procedure is repeated for different c, and one obtains the desired chemokinetic dose-response curve (Fig. 2). The oscillation amplitude of M increases with increasing amplification factor. The more realistic model predicts a threshold for small c. The oscillation amplitude of M is zero for $c < c_c$ and finite for $c > c_c$. This threshold behavior is an essential difference between the prediction of the simple and of the more realistic model. The critical concentration, c_c, alters when the amplification is altered. The measured chemokinetic dose-response curve is compared to the calculated curve (Fig. 2). The systematic deviations between the measured and the predicted values are evident at low concentration ($c < K_R$). The measured speed is larger than the predicted one. This systematic deviation can partially be explained by systematic errors in the experimental determination of the speed. (i) The cells are washed but it is possible that kinesis-stimulating molecules of the blood plasma are attached at the cells. (ii) The translocation of the center of mass of a migrating cell is determined from the center of the cellular contour line. For low speeds, this approximation can lead to considerable error, for example when a change of the cellular contour occurs without net displacement. (iii) A further systematic error originates from immobile cells (a certain fraction of the cells do not move). This fact can be explained by nonidentical biological objects (e.g., cellular age), preparation artifacts (e.g., injured cells). In general, the mean speed is calculated without considering immobile cells. But this leads to a too large value at low c since the fraction of immobile cells increases with decreasing c [1–3 % of immobile cells at large c ($> K_R$) and 20–30 % at low c ($< K_R$)]. When the measured speed is corrected, the accordance is better than that shown here. New experiments are in preparation to clarify this point.

Cell migration, surface instability, and laser

It is interesting to note that the speed of stimulated cells can be compared with the stimulated light emission of a laser. Both systems are far from thermodynamic equilibrium. The essential parameter for a laser is the light pump energy and the essential parameter for a cell is the concentration of migration-stimulating molecules which activate the cellular signal transduction chain. There exists a critical value for each example; if the parameter is below a critical value, then the output of the system is zero—no coherent light leaving the laser, the cellular signal chain does not perform oscillation. If the parameter is above a critical value, then the output of the system is nonzero. Coherent light is leaving the laser and its intensity increases with increasing pump energy. The cellular signal chain performs oscillations and the amplitude increases with increasing concentration of the cell-stimulating molecules.

Direct conversion of chemical into mechanical energy and signal transduction in self-organized entities is one of the main processes in biological movements. The signal transduction chain of granulocytes can also be interpreted as an interfacial instability [5]. Nakache and Dupeyrat [33] investigated the spontaneous motions of model systems where a surface instability takes place. The movements occur between two immiscible solutions containing charged species, one of which is surface-active and, therefore, modifies the interfacial tension between the two media. Periodic motions in the interface plane take place when an aqueous solution of long-chain alkyltrimethylammonium halogenide is poured over a nitrobenzene solution. These large-scale interfacial motions are attributed to the Marangoni effect where interfacial flow is driven by gradients in interfacial tension due to concentration variations resulting from mass transfer through the interface. If, for example, a 2 mm large drop of one phase is surrounded by the other one, it is propelled by jumps [5]. Thus, a droplet is driven to migrate by a surface instability. The movement can be directed by light if a copolymer is introduced into the interface [5]. The surface tension of the copolymer (methyl methacrylate and spiropyran derivative) is altered by light [34]. The interfacial instability will start in a part that is illuminated with UV light. The migration distance is very small since the droplets are far from thermodynamic equilibrium only briefly.

Outlook

A common concept for understanding systems far from thermodynamic equilibrium is consequently applied to cell migration. This study wants to place the migration of cells in a better perspective. Here, the chemokinetic response is analyzed in detail. The signal transduction chain for directed phenomena can be treated in a similar but more complex way. In addition, the description is not restricted to granulocytes. It should hold for cells such as monocytes, fibroblasts, osteoblasts, keratinocytes, and neural crest cells. Other phenomena where feedback and delayed signals are essential in the signal transduction chain can be investigated in a similar way, e.g., nerve growth.

The practical importance of this study lies in the detailed analysis of the experimental condition. The description may be useful in the definition of cellular dysfunction. For example, virus-induced disturbances where the temporal and spatial events in the signal transduction chain are altered [35].

The emphasis on the current research is to go beyond this machine description. The cell regarded as a self-organized molecular machine raises many questions about the involved physical laws. At present state the physical aspects of the cellular signal transduction chain are focused into a typical liquid crystal problem—the vesicle fusion process.

ACKNOWLEDGMENTS

We are grateful to Professor Jean Bernard (Academie Française), Professor Jaques-Louis Binet, and Dr. Anne de Boisfleury-Chevance (Centre d'Écologie Cellulaire) for their support and encouragement. One of us. (M.S.)

thanks the Deutsche Forschungsgemeinschaft. One of us (H.G.) is grateful to the Fondation de France for honoring him and for giving him the opportunity to work in Paris.

APPENDIX A: GENERAL SOLUTION

The general solution of Eq. (10),

$$\frac{d}{dt}\begin{bmatrix} R \\ R_C \end{bmatrix} = \begin{bmatrix} a_{11} & a_{12} \\ a_{21} & a_{22} \end{bmatrix} \begin{bmatrix} R \\ R_C \end{bmatrix} + \begin{bmatrix} f(M) \\ 0 \end{bmatrix}, \tag{A1}$$

is

$$\begin{bmatrix} R \\ R_C \end{bmatrix} = \int_0^t \exp[\,\mathbf{A}(t-t')] \begin{bmatrix} f(M) \\ 0 \end{bmatrix} dt' \tag{A2}$$

(A3)

with

$$\mathbf{A} = \begin{bmatrix} a_{11} & a_{12} \\ a_{21} & a_{22} \end{bmatrix}, \tag{A4}$$

$$\exp[\,\mathbf{A}(t-t')] = (\exp[\lambda_1 t]\mathbf{B}_1 + \exp[\lambda_2 t]\mathbf{B}_2)\mathbf{B}^{-1}, \tag{A5}$$

$$\mathbf{B}_1 = (\,\mathbf{A} - \lambda_2 \mathbf{E}), \tag{A6}$$

$$\mathbf{B}_2 = (\,\mathbf{A} - \lambda_1 \mathbf{E}), \tag{A7}$$

$$\mathbf{B} = \mathbf{B}_1 + \mathbf{B}_2 . \tag{A8}$$

The **B** values are by using the eigenvalues $\lambda_{1/2}$ [Eq. (49)]:

$$\mathbf{B}_1 = \begin{bmatrix} a_{12} & a_{12} \\ a_{21} & a_{21} \end{bmatrix}, \tag{A9}$$

$$\mathbf{B}_2 = \begin{bmatrix} -a_{21} & a_{12} \\ a_{21} & -a_{12} \end{bmatrix}, \tag{A10}$$

$$\mathbf{B}^{-1} = \frac{1}{a_{12}^2 - 2a_{12}a_{21} - a_{12}^2} \begin{bmatrix} a_{12}-a_{21} & 2a_{21} \\ 2a_{12} & a_{21}-a_{12} \end{bmatrix}. \tag{A11}$$

The final result is the temporal changes of the number of receptors, $R(t)$,

$$R(t) = \int_0^t \left[\frac{a_{21}\exp[\lambda_1(t-t')] + a_{12}\exp[\lambda_2(t-t')]}{a_{12}+a_{21}} \right] f(M)dt' , \tag{A12}$$

and the temporal changes of the number of occupied receptors, $R_C(t)$,

$$R_C(t) = \int_0^t \left[\frac{a_{21}\exp[\lambda_1(t-t')] - a_{21}\exp[\lambda_2(t-t')]}{a_{12}+a_{21}} \right] f(M)dt' . \tag{A13}$$

APPENDIX B: ADIABATIC APPROXIMATION

A part of the integration in Eqs. (13) and (14) can be performed if the receptor supply function, $f(M)$, varies slowly in time compared with the exponential function $\exp[\lambda_1 t]$:

$$R(t) = f(M)\frac{a_{21}}{a_{12}+a_{21}}\frac{(1-\exp[\lambda_1 t]}{\lambda_1} + \frac{a_{12}}{a_{12}+a_{21}}\int_0^t \exp[\lambda_2(t-t')]f(M(t'))dt' . \tag{B1}$$

A Taylor series of $f(M(t'))$ is taken to proceed further:

$$F(M(t')) = f(M(t)) - \frac{df}{dt}(t-t') + \frac{1}{2}\frac{d^2f}{dt^2}(t-t')^2 \mp \cdots . \tag{B2}$$

The remaining integral can be solved in the following way:

$$\begin{aligned} \int_0^t \exp[\lambda_2(t-t')]f(M(t'))dt' &= f(M)\int_0^t \exp[\lambda_2(t-t')]dt' - \frac{df}{dt}\int_0^t \exp[\lambda_2(t-t')](t-t')dt' \\ &\quad + \frac{d^2f}{dt^2}\int_0^t \exp[\lambda_2(t-t')]\frac{(t-t')^2}{2}dt' - \cdots \\ &= \frac{f(M)}{\lambda_2}P(1,-\lambda_2 t) - \frac{\dot{f}}{\lambda_2^2}P(2,-\lambda_2 t) + \frac{\ddot{f}}{\lambda_2^3}P(3,-\lambda_2 t) - \cdots , \end{aligned} \tag{B3}$$

where $P(n,t)$ is the incomplete gamma function of order n (Fig. 7):

$$P(n,t)=\int_0^t \exp[-t']\frac{(t')^{n-1}}{(n-1)!}dt' . \tag{B4}$$

The higher-order terms in (B3) can be neglected if λ_2 is in the order of $\dot{f}$. One gets

$$\int_0^t \exp[\lambda_2(t-t')]f(\boldsymbol{M}(t'))dt' \approx \frac{f(M)}{\lambda_2}P(1,-\lambda_2 t) = \frac{f(M)}{\lambda_2}(1-\exp[\lambda_2 t]) . \tag{B5}$$

The temporal variations of the receptor density, $R(t)$, are obtained by inserting this result in (B1):

$$R(t)=\frac{f(M)}{2k_e}\frac{k_{22}+k_e}{k_{22}+k_{11}c} -f(M)\left[\frac{a_{21}}{a_{12}+a_{21}}\frac{\exp[\lambda_1 t]}{\lambda_1} +\frac{a_{12}}{a_{12}+a_{21}}\frac{\exp[\lambda_2 t]}{\lambda_2}\right] . \tag{B6}$$

If the receptor ligand binding process is fast (large λ_1) and the receptor inactivation process (small λ_2) then the final result is

$$R(t)=\frac{f(M)}{2k_e}\frac{k_{22}+k_e}{k_{22}+k_{11}c}-f(M)\frac{a_{12}}{a_{12}+a_{21}}\frac{\exp[\lambda_2 t]}{\lambda_2} . \tag{B7}$$

The same calculation can be performed for $R_C(t)$.

APPENDIX C: CHEMICAL AMPLIFIER AND FOCKER-PLANCK EQUATION

The rate equations of the chemical amplification chain

$$\dot{S}_i=-(f_1+b_1)S_1+b_2S_2 , \tag{C1}$$

$$\dot{S}_i=-(f_i+b_i)S_i+f_{i-1}S_{1-1}+b_{i+1}S_{i+1} \tag{C2}$$

$$\text{for } i=2,\ldots,N-1 , \tag{C3}$$

$$\dot{S}_N=-(f_N+b_N)S_N+f_{N-1}S_{N-1} \tag{C4}$$

can be transformed into a Fokker-Planck equation. This approximation is valid for large N. The connection between the suffix, i, of the rate equations and a continuous state variables, x, is

$$x=2\pi\frac{i}{N} . \tag{C5}$$

The rate equation with the continuous state variable is then

$$\dot{S}(x)=f(x-\epsilon)S(x-\epsilon)-f(x)S(x) +b(x+\epsilon)S(x+\epsilon)-b(x)S(x) , \tag{C6}$$

where ϵ is a small increment of the state variable x. In the next step, a Taylor series of S with respect to x is taken:

$$S(x-\epsilon)=S(x)-\epsilon\frac{\partial S}{\partial x}+\frac{\epsilon^2}{2}\frac{\partial^2 S}{\partial x^2}\pm\cdots , \tag{C7}$$

$$S(x+\epsilon)+S(x)+\epsilon\frac{\partial S}{\partial x}+\frac{\epsilon^2}{2}\frac{\partial^2 S}{\partial x^2}+\cdots . \tag{C8}$$

A differential equation—the Fokker-Planck equation—is obtained by inserting these Taylor series into Eq. (C6):

$$\frac{\partial S}{\partial t}=\frac{\partial}{\partial x}\left\{-F(x)+\frac{\partial}{\partial x}D(x)\right\}S(x) \tag{C9}$$

with the drift term

$$F(x)=\epsilon[f(x)-b(x)] \tag{C10}$$

and the diffusion term

$$D(x)=\tfrac{1}{2}\epsilon^2[f(x)+b(x)] . \tag{C11}$$

The drift term $F(x)$ describes how fast the chemical reactions penetrate through the chemical amplifier. (F^{-1} is proportional to the time.) The diffusion term, $D(x)$, describes the broadening of the input signal. If the forward and backward rate constants are the same for every step [$f(x)=f, b(x)=b$], Eq. (C9) simplifies to

$$\frac{\partial S}{\partial t}=-F\frac{\partial S}{\partial x}+D\frac{\partial^2 S}{\partial x^2} \tag{C12}$$

with

$$F=\epsilon(f-b) , \tag{C13}$$

$$D=\tfrac{1}{2}\epsilon^2(f+b) . \tag{C14}$$

APPENDIX D: LINEARIZATION OF THE SIGNAL TRANSDUCTION CHAIN

The signal transduction chain is described by differential equation (34). The integral of this equation can be approximated if $G(t-t')$ is expanded in a Taylor series in respect to t:

$$G(t-t')=G(t)\frac{dG}{dt}t'+\frac{1}{2}\frac{d^2G}{dt^2}t'^2\mp\cdots \tag{D1}$$

with

$$\frac{dG}{dt}=\frac{\partial G}{\partial M}\frac{dM}{dt} , \tag{D2}$$

$$\frac{d^2G}{dt^2}=\frac{\partial^2 G}{\partial M^2}\frac{dM}{dt}+\frac{\partial G}{\partial M}\frac{d^2M}{dt^2} . \tag{D3}$$

Then, $G(t)$ is regarded near the steady state and a Taylor series in respect to m is made

$$G(t)=G(M_0)+\left.\frac{\partial G}{\partial M}\right|_{M_0}(M-M_0)+\cdots . \tag{D4}$$

Equations (D2)–(D4) are inserted into Eq. (D1). One obtains

$$G(t-t')=G(M_0)+\left.\frac{\partial G}{\partial M}\right|_{M_0}(M-M_0)+\frac{\partial G}{\partial M}\left[-\frac{dM}{dt}t'+\frac{1}{2}\frac{d^2M}{dt^2}t'^2\right]\cdots \quad \text{(D5)}$$

if only terms up to $\partial G/\partial M$ are considered. The integral of Eq. (34) then reads

$$\frac{1}{(N-1)!}\int_0^t t'^{(N-1)}e^{-t'}[G_0+G_0'm(t-t')]dt' = G_0P(N,t)+G_0'\left[mP(N,t)-\frac{dm}{dt}NP(N+1,t)+\frac{1}{2}\frac{d^2m}{dt^2}N(N+1)P(N+2,t)\right] \quad \text{(D6)}$$

with $m=M-M_0$. The incomplete gamma function $P(N,t)$ is approximated by the step function $\Theta(t-N)$. The bracket of this equation is approximated by

$$\Theta(t-N)\left[m-\frac{dm}{dt}N+\frac{1}{2}\frac{d^2m}{dt^2}N^2\right] \quad \text{(D7)}$$

by using $\Theta(t-N)\approx\Theta(t-N-1)\approx\Theta(t-N-2)$ and $N(N+1)\approx N^2$. The bracket of Eq. (D7) is a Taylor series of $m(t-N)$ with respect to N.

The same result is obtained if the Poisson distribution on the right-hand side of Eq. (D6) is approximated by Dirac's delta function, $\delta(t)$. The approximation for the bracket of Eq. (D6) is then

$$\int_0^t\delta(t'-N)m(t-t')dt' . \quad \text{(D8)}$$

The integration can be performed and one obtains $m(t-N)$.

The brackets of Eq. (D6) can be approximated by

$$mP(N,)-\frac{dm}{dt}NP(N+1,t)+\frac{d^2m}{dt^2}N(N+1)(N+2) \approx m(t-N) \text{ for } t>N \quad =0 \text{ for } t<N .$$

The linearized differential equation for the signal transduction chain is

$$f_0\frac{dm}{dt}=G_0P(N,t)+\left.\frac{\partial G}{\partial M}\right|_{M_0}m(t-N)-\left[H_0+\left.\frac{\partial H}{\partial M}\right|_{M_0}m(t)\right] . \quad \text{(D9)}$$

[1] P. C. Wilkinson, *Chemotaxis and Inflammation* (Churchill, London, 1974).
[2] J. P. Trinkaus, *Cells into Organs* (Prentice-Hall, Englewood Cliffs, NJ, 1984).
[3] H. Haken, *Synergetics* (Springer, Berlin, 1983).
[4] H. Gruler and A. de Boisfleury-Chevance, J. Phys. (France) I **4**, 1085 (1994).
[5] H. Gruler, in *Chaos and Complexity,* edited by J. T. Thanh Van (Editions Frontières, Gif sur Yvette, 1994).
[6] A. Mikhailov, in *Evolution of Dynamical Structures in Complex Systems,* edited by R. Friedrich and A. Wunderlin (Springer, Berlin, 1992).
[7] H. Gruler, in *Biologically Inspired Physics,* edited by L. Peliti (Plenum, New York, 1991).
[8] M. Schienbein, K. Franke, and H. Gruler, Phys. Rev. E **49**, 5462 (1994).
[9] S. Malawista, Ann. N.Y. Acad. Sci. **466**, 858 (1988).
[10] H. Gruler and A. de Boisfleury-Chevance, Z. Naturforsch. C **42**, 1126 (1987).
[11] M. Schienbein and H. Gruler, Bull. Math. Biol. **55**, 585 (1993).
[12] N. Wiener, *Cybernetics: Or Control and Communication in Animal and the Machine* (MIT, Cambridge, 1961).
[13] *The Cellular Biochemistry and Physiology of Neutrophil,* edited by M. B. Hallett (Chemical Rubber, Boca Raton, 1989).
[14] E. L. Becker, Y. Kanaho, and J. C. Kermode, Biomed. Pharmacother. **41**, 289 (1987).
[15] D. A. Lauffenburger and J. J. Linderman, *Receptors Models for Binding, Trafficking, and Signaling* (Oxford University Press, New York, 1993).
[16] R. T. Tranquillo and D. A. Lauffenburger, J. Math. Biol. **25**, 229 (1987).
[17] H. Gruler, in *Biological Motion,* edited by W. Alt and G. Hoffmann, Lecture Notes in Biomathematics (Springer, Heidelberg, 1990).
[18] V. Vereycken, H. Gruler, C. Bucherer, C. Lacombe, Y. Zerrouki, and J-C. Lelièvre, J. Phys. (France) III (to be published).
[19] G. Gerisch and H-U. Keller, J. Cell Sci. **52**, 1 (1981).
[20] K. Franke and H. Gruler, Eur. Biophys. J. **18**, 335 (1990).
[21] K. Franke and H. Gruler, Z. Naturforsch. C **49**, 241 (1994).
[22] U. Jäger, H. Gruler, and B. Bültmann, Klin. Wochenschr. **66**, 434 (1988).
[23] R. S. Hartman, K. Lau, W. Chou, and T. D. Coates, Biophys. J. **67**, 2535 (1994).
[24] M. P. Wymann, P. Kernen, T. Bengtsson, M. Baggiolini, and D. A. Derauleau, J. Biol. Chem. **265**, 619 (1990).
[25] M. U. Ehrengruber, T. D. Coates, and D. A. Derauleau, FEBS Lett. (to be published).
[26] J. Wilschut and D. Hoekstra, *Membrane Fusion* (Dekker, New York, 1991).
[27] H. Segel, *Biochemical Calculations* (Wiley, New York, 1976).
[28] A. Goldbeter, G. Dupond, and M. Berridge, Proc. Natl. Acad. Sci. USA **87**, 1641 (1990).
[29] A. Y. K. Wong, A. Fabiato, and J. B. Bassingthwaigthe, Bull. Math. Biol. **54**, 95 (1992).
[30] J. D. Murray, *Mathematical Biology* (Springer-Verlag, Berlin, 1989).
[31] S. Weis, Dipolomarbeit, Universität Ulm, 1994.

[32] M. Schienbein, A. de Boisfleury-Chevance, and H. Gruler (unpublished).
[33] E. Nakache and M. Dupeyrat, J. Colloid. Interface Sci. **94**, 187 (1983).
[34] H. Gruler, R. Vilanove, and F. Rondelez, Phys. Rev. Lett. **44**, 590 (1980).
[35] B. D. Bültmann and H. Gruler, J. Cell Biol. **96**, 1708 (1983).
[36] E. L. Becker, H. J. Showewll, P. H. Naccache, and R. Sha'afi, in *Chemotaxis Leukocytes,* edited by J. I. Gallin and P. G. Quie (Raven, New York, 1978).
[37] H. Gruler, in *Immunochemical Techniques Part L: Chemotaxis and Inflammation,* edited by G. Di Sabato, Methods in Enzymology Vol. 162 (Academic, New York, 1988).